

New lithium-ion conducting compounds $3\text{Li}_3\text{N-MI}$ ($\text{M} = \text{Li}, \text{Na}, \text{K}, \text{Rb}$) and their application to solid-state lithium-ion cells

Shinji Hatake, Jun Kuwano *, Makoto Miyamori, Yasukazu Saito, Satoshi Koyama

Department of Industrial Chemistry, Faculty of Engineering, Science University of Tokyo, 1-3 Kagurazaka, Shinjuku-ku, Tokyo 162, Japan

Accepted 3 March 1997

Abstract

In the quasi-binary systems $\text{Li}_3\text{N-MI}$ ($\text{M} = \text{Li}, \text{Na}, \text{K}, \text{Rb}$) new intermediate compounds $3\text{Li}_3\text{N-MI}$ were synthesized by a solid-state reaction between Li_3N and MI at 600°C . They were isomorphous and had a tetragonal unit cell. Their sintered bodies exhibited lithium-ion conductivity of 1.1×10^{-4} – $7.0 \times 10^{-5} \text{ S cm}^{-1}$ at room temperature. The grain boundary resistances were negligibly small because of their good sinterability. The decomposition voltages were approximately 2.5–2.8 V, much higher than that of Li_3N . Even the compacts of the powdered compounds showed total conductivities more than $10^{-5} \text{ S cm}^{-1}$. This allowed the cell construction of the solid-state lithium-ion cell, $\text{C}/3\text{Li}_3\text{N-KI}/\text{LiTiS}_2$, simply by pressing the powdered electrolyte and electrode materials. The cell was able to charge and to discharge at a constant current of $15 \mu\text{A cm}^{-2}$ at room temperature; however, severe polarization in the positive electrodes limited the charge/discharge performance. © 1997 Elsevier Science S.A.

Keywords. Lithium. Solid electrolytes, Carbon; Lithium-ion cells; Rocking-chair batteries; Intercalation

1. Introduction

The use of metallic lithium as an anode and lithium intercalation compounds as a cathode leads to attractive battery systems with a high energy density, because of the low equivalent weight of Li and a large free energy change involved in the cell reaction. Demands for high energy density batteries have rapidly grown and 3 V Li systems based on non-aqueous electrolytes, such as Li/MnO_2 and Li/MoS_2 , have expanded their use for the last fifteen years. However, Li-rechargeable systems have encountered serious problems arising from the dendritic deposition of Li during discharge and its high reactivity. To alleviate this problem, novel Li-rechargeable cells using carbon–lithium intercalation compounds as the anode material have been recently developed and commercialized [1–6]. They are called ‘rocking-chair cell’ or ‘lithium-ion cell’ because of the innovative mechanism and performance. They bring numerous advantages over Li metal, most notably in safety, cost, charge/discharge cycle characteristics and flexibility in cell design.

To date, organic electrolytes have been practically used in the commercially available batteries. However, the electrolyte is not always necessary to be based on organic solvents which may cause serious problems such as its leakage and

combustion, self-discharge, and even explosion of the decomposed products in very rare cases. Solid electrolytes would be a possible replacement for the electrolytes, with which we may expect several advantages over liquid-electrolyte counterparts, i.e., safety operation, long shelf life, wide operating temperature range, ease of miniaturization, etc.

Furthermore, for the solid-state Li cells, carbon-based materials are more attractive, because, unlike Li metal, they are expected to show relatively good compatibility with polycrystalline electrolytes allowing intimate interfacial contact with a large interface area, simply by mixing with polycrystalline electrolyte and pressing the mixture.

Among representative families of polycrystalline Li electrolytes based on oxides are $\gamma_{\text{II}}\text{-Li}_3\text{PO}_4$ -type solid solutions [7,8], Li-substituted NASICONs [9,10], and A-site deficient perovskites [11,12]. Despite their high intragranular (bulk) conductivity, they exhibit rather lower total conductivity after sintering, still much lower conductivity without sintering. Thus, they unlikely show good compatibility with polycrystalline electrode materials without sintering.

Li_3N [13–15] has a bulk conductivity as high as $10^{-3} \text{ S cm}^{-1}$ at room temperature, while the low decomposition voltage, 0.45 V, and the difficulty in sintering prevent its application. Several quasi-binary and -ternary compounds such as Li_5NI_2 have been synthesized to alleviate the draw-

* Corresponding author. Tel.: +813-3260-4271, Fax. +813-5261-4631

backs [16,17]. Furthermore, we expect that the incorporation of large, deformable iodide ions bring the merits: the resultant electrolyte shows good compatibility with electrode materials, and the total conductivity of the as-pressed compact is not much lower than the bulk conductivity. This would allow cell construction without sintering by cold-pressing the electrolyte and electrode mixtures, as with solid-state cells using silver and copper halide-based electrolytes [18].

This paper describes the synthesis of new intermediate compounds in the quasi-binary systems $\text{Li}_3\text{N-MI}$ ($\text{M} = \text{Li, Na, K, Rb}$), together with their electrical and electrochemical properties. In addition, we also present preliminary results on the solid-state Li-ion cell, $\text{C}/3\text{Li}_3\text{N-KI}/\text{LiTiS}_2$, which was constructed simply by pressing the constituent powders.

2. Experimental

All chemicals used were reagent grade (Wako Pure Chemical). Li_3N was synthesized by a direct reaction of Li lumps (>99%) with pure nitrogen gas (five nine) of 1.2 MPa in a pressure-proofed stainless-steel vessel, followed by annealing at about 85°C. The lumps of Li_3N were crushed in a stainless-steel mortar and finely ground in an alumina mortar. Intimate mixtures of the powdered Li_3N and MI ($\text{M} = \text{Li, Na, K, Rb}$) were uniaxially pressed into pellets (12 mm in diameter and 1.5–2 mm thick) at 300 MPa. Each pellet was wrapped in a nickel foil, sealed in a silica tube under a nitrogen atmosphere and reacted at a temperature of 500–700°C for 24 h. The products were reground prior to the use described below.

A conductivity measurement cell was made by d.c. sputtering gold onto the opposite faces of the as-prepared (sintered) pellet after removing a surface layer with lapping films. Another cell was made with the ground product similarly by pressing and sputtering to compare the conductivity of the compact with that of the as-prepared pellet. The cell was placed between the gold electrodes of a conductivity jig, which was put in a Pyrex tube. The temperature of the cell was controlled within $\pm 0.05^\circ\text{C}$ in a range of -30 to 150°C with a programmable oil-bath and within $\pm 0.15^\circ\text{C}$ in a range of 150 – 300°C with an electric furnace. The a.c. impedance data were collected with an impedance analyser (YHP 4192A) over the frequency range, $f = 5$ Hz–13 MHz and analysed in three interrelated formalisms [19], the complex impedance (Z^*), the complex admittance (Y^*), the complex modulus (M^*) to estimate bulk and total conductivity. Powder X-ray diffraction analysis was made with a Rigaku RAD-C system (Ni-filtered $\text{Cu K}\alpha$) and the Cell-series programs [20].

The positive electrode material TiS_2 were synthesized by a solid-state reaction between Ti and S, and LiTiS_2 , by treatment of TiS_2 with *n*-butyllithium, according to the methods described in the literature [21,22]. The cells of the type, Li foil (1 mm)/E (0.1 g)/ TiS_2 (0.1 g) (E: $3\text{Li}_3\text{N-MI}$, $D = 1$ cm), were assembled and discharged across a constant load

of $1 \text{ M}\Omega$ at 25°C to estimate the transference numbers of the Li ion in the electrolytes approximately. The Li-ion cell, C,E/E/ LiTiS_2 ,E ($D = 7$ mm, $L = \sim 1$ mm, C: natural graphite NG-7, Kansai Cork Chemicals, E: $3\text{Li}_3\text{N-KI}$), with a theoretical capacity of 2.64 mAh (negative electrode capacity) was also constructed by pressing the electrolyte (42 mg) and the electrode mixtures (negative electrode: 7 mg C + 7 mg E, positive electrode: 35 mg LiTiS_2 + 8.4 mg E) at 300 MPa. An Li reference electrode ($D = 2$ mm) was also attached beside the carbon electrode to examine the polarization behavior of the negative and positive electrodes.

The cells of the type, Li/as-prepared pellet (0.2 g)/Au plate ($D = 2$ mm), were also made for measurements of their decomposition voltages. Charge/discharge tests and electrochemical measurements were carried out with a potentiostat (Hokuto Denko, HA-501) and electrometers (Hokuto Denko, HE-104). All the experiments which required avoiding humidity and air were carried out under a dry atmosphere of argon or nitrogen.

3. Results and discussion

The optimal reaction temperature was 600°C in the solid-state reaction between Li_3N and MI: the reaction did not complete at 550°C , while the mixtures reacted considerably with the Ni-foils above 650°C . X-ray diffraction analysis showed that a single phase formed at the same composition $3\text{Li}_3\text{N-MI}$ in each system. The samples were mixtures containing Li_3N on the Li_3N -rich side and those containing MI on the MI-rich side.

The yellow products of $3\text{Li}_3\text{N-MI}$ ($\text{M} = \text{Li, Na, K, Rb}$) exhibited very similar X-ray diffraction patterns except for slight changes in peak position and intensity. All the reflections were indexed in a tetragonal unit cell for all the intermediate compounds, indicating that a new family of the isomorphous compounds was formed. Table 1 lists the crystal data including their lattice constants (a , c) and the most probable space group selected by the Cell-series programs.

For the as-prepared (sintered) pellets of the $3\text{Li}_3\text{N-MI}$ compositions, all the complex impedance plots gave a nearly perfect semicircle, due to the response of the bulk part, with a low-frequency spike due to the response of the blocking gold electrode–electrolyte interface, as with a single crystal. This indicated that the total conductivities were equal to the bulk conductivities on account of the negligibly small grain boundary resistances, and that the intermediate compounds

Table 1
Crystal data for the intermediate compounds $3\text{Li}_3\text{N-MI}$

Composition	Crystal system	Space group	Lattice parameter
$3\text{Li}_3\text{N-LiI}$	Tetragonal	$I4_1/amd$	$a = 7.339$ $c = 10.374$
$3\text{Li}_3\text{N-NaI}$	Tetragonal	$I4_1/amd$	$a = 7.327$ $c = 10.362$
$3\text{Li}_3\text{N-KI}$	Tetragonal	$I4_1/amd$	$a = 7.329$ $c = 10.364$
$3\text{Li}_3\text{N-RbI}$	Tetragonal	$I4_1/amd$	$a = 7.331$ $c = 10.367$

had good sinterability. The parallel capacitances associated with the semicircles were $5\text{--}8 \times 10^{-12}$ F, being reasonable magnitude for the bulk response in view of the geometrical factors of cell. Table 2 lists the total (bulk) conductivities of the $3\text{Li}_3\text{N-MI}$ compounds, which are high, 1.1×10^{-4} – 7.0×10^{-5} S cm^{-1} at room temperature. From a practical point of view, total conductivity is more important than bulk conductivity. No oxide-based conductors with a better total conductivity than that of this family have been so far known. Apart from amorphous materials, the total conductivity is rivaled only with those of Li_3N [13–15] and $\text{Li}_3\text{N-LiOH-LiI}$ [17]; however, their decomposition potentials have been reported to be 0.45 and ~ 1.6 V, respectively.

Fig. 1 shows the Arrhenius plots of conductivity for the intermediate compounds, indicating that the plots follow the Arrhenius equation well. No changes in the slopes are observed, suggesting that the intermediate compounds are stable in the temperature range from -20 to 300°C . The activation energies, ΔH , for Li-ion conduction were 0.32–0.43 eV, calculated over the same temperature range. The pre-exponential factors, σ_0 , are listed in Table 2, together with ΔH . Interestingly, the $3\text{Li}_3\text{N-LiI}$ compound are larger in ΔH , σ_0 , a , and c than the others.

For the as-pressed compacts of the intermediate compounds, the complex impedance plots showed a single but deformed semicircle. The associated parallel capacitances, $3\text{--}7 \times 10^{-11}$ F, were somewhat larger than those for the bulk

semicircles of the as-prepared pellets. The distortion probably results from the overlap of the bulk response with the response due to grain boundary or/and a polluted layer. All the compacts still maintained total conductivities higher than 10^{-5} S cm^{-1} at room temperature, as listed in Table 2. We also prepared the as-pressed compact and as-prepared pellets of the powdered Li_3N under the same preparation conditions as those for the $3\text{Li}_3\text{N-MI}$ electrolytes. The bulk conductivities of both were about 10^{-3} S cm^{-1} at room temperature, while the total conductivities were low, 1.0×10^{-6} S cm^{-1} for the as-pressed pellet and 2.1×10^{-6} S cm^{-1} for the as-prepared pellet. The incorporation of iodide ions thus brought the merit that the as-pressed compacts had not much lower conductivities than own bulk conductivities without sintering, unlike oxide-based electrolytes and Li_3N .

The $\text{Li}/3\text{Li}_3\text{N-MI}/\text{TiS}_2$ cells had open-circuit voltages of 2.51–2.56 V at 25°C and were capable of delivering continuous currents more than $2.5 \mu\text{A cm}^{-2}$ across a constant load $1 \text{ M}\Omega$, keeping cell voltages more than 2.2 V for at least 10 h. This revealed that the Li transference numbers in the intermediate compounds were almost unity. The decomposition voltages of the $3\text{Li}_3\text{N-MI}$ compounds were approximately 2.5–2.8 V, much higher than those of Li_3N and the $\text{Li}_3\text{N-LiOH-LiI}$ electrolyte. The results are summarized in Table 3.

The as-assembled cell $\text{C}/3\text{Li}_3\text{N-KI}/\text{LiTiS}_2$ was initially charged up to 10% of the theoretical cell capacity at a constant current of $10 \mu\text{A cm}^{-2}$ and then discharged at a constant current of $15 \mu\text{A cm}^{-2}$ to a cutoff voltage of 1.0 V. After that, the cell was subjected to charge/discharge cycling tests, because the charge/discharge characteristics were considerably bad without this pretreatment. The depth of charge was about 7% of the theoretical cell capacity at the start of the first cycle. Fig. 2 shows the charge/discharge curves of the Li-ion cell, $\text{Li}_6\text{C}_6/3\text{Li}_3\text{N-KI}/\text{LiTiS}_2$, demonstrating that the cell works as an Li-ion cell. The coulombic efficiency was 87% at the first cycle. The charge/discharge characteristics remained almost unchanged at the 10th cycle; the coulombic efficiency was 89%. The results illustrate that the cold-pressed compact of the $3\text{Li}_3\text{N-KI}$ powder can be used without sintering the electrolyte in Li-ion microcells.

The polarization behavior in the cell was examined to know which electrode is more responsible for the polarization during the charge/discharge cycle. Fig. 3 shows the polarization curves of both electrodes which were measured immediately

Table 2
Conductivity data of the intermediate compounds $3\text{Li}_3\text{N-MI}$ ^a

Composition	$\sigma(t)$ (S cm^{-1})	$\log(\sigma_0)$ ($\text{S cm}^{-1} \text{K}$)	ΔH (eV)	$\sigma(p)$ (S cm^{-1})
$3\text{Li}_3\text{N-LiI}$	7.0×10^{-5}	5.59	0.43	2.3×10^{-5}
$3\text{Li}_3\text{N-NaI}$	9.1×10^{-5}	4.19	0.34	2.1×10^{-5}
$3\text{Li}_3\text{N-KI}$	1.0×10^{-4}	4.23	0.34	1.5×10^{-5}
$3\text{Li}_3\text{N-RbI}$	1.1×10^{-4}	3.93	0.32	1.8×10^{-5}

^a $\sigma(t)$: total (bulk) conductivity at 25°C of the as-prepared pellets; σ_0 : pre-exponential factor calculated from the Arrhenius plots; ΔH : activation energy for Li conduction; $\sigma(p)$: total conductivity at 25°C of the as-pressed pellets

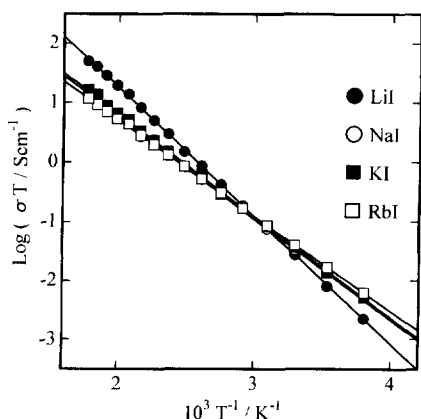


Fig. 1 Arrhenius plots of ionic conductivity for intermediate compounds $3\text{Li}_3\text{N-MI}$ ($M = \text{Li, Na, K, Rb}$).

Table 3
Electrochemical properties of the intermediate compounds $3\text{Li}_3\text{N-MI}$ ^a

Composition	V_d (V)	V_{OCV} (V)	V_{dis} (V)
$3\text{Li}_3\text{N-LiI}$	2.6–2.7	2.52	2.3
$3\text{Li}_3\text{N-NaI}$	2.6–2.7	2.51	2.3
$3\text{Li}_3\text{N-KI}$	2.5–2.6	2.53	2.25
$3\text{Li}_3\text{N-RbI}$	2.5–2.6	2.56	2.25

^a V_d : decomposition voltage; V_{OCV} : open-circuit voltage at 25°C of the Li/TiS_2 cell; V_{dis} : cell voltage after discharge for 10 h at a constant load of $1 \text{ M}\Omega$ at 25°C .

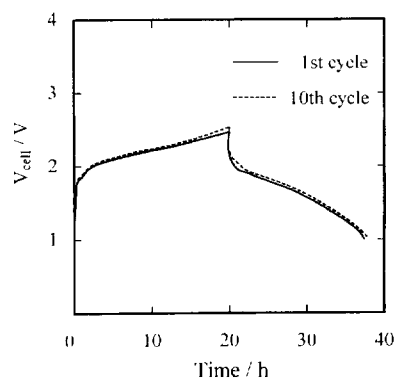


Fig. 2. Charge/discharge curves at a constant current of $15 \mu\text{A cm}^{-2}$ for the solid-state Li-ion cell, $\text{C}/3\text{Li}_3\text{N-KI}/\text{LiTiS}_2$, at 25°C . Cutoff voltage 1.0 V (discharge); 2.46 V (charge at the 1st cycle), and 2.53 V (charge at the 10th cycle).

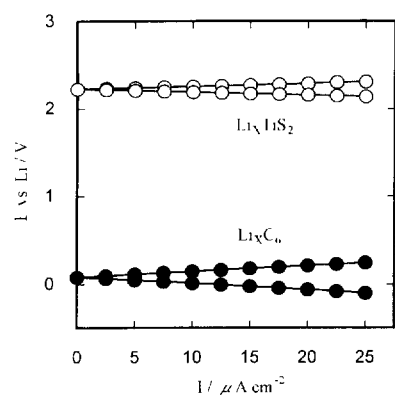


Fig. 3. Polarization curves of both electrodes for the solid-state Li-ion cell, $\text{C}/3\text{Li}_3\text{N-KI}/\text{LiTiS}_2$, at 25°C .

after the charge (cutoff voltage: 2.55 V) at the 11th cycle. The anodic polarization was very similar to the cathodic polarization both for the Li_3TiS_2 and Li_xC_6 electrodes. Although the polarization of both electrodes was not serious, the polarization of the Li_xC_6 electrode was twice larger than that of the Li_3TiS_2 electrode both in anodic and cathodic directions. When the cell was on open circuit, the potential of the electrode was always more positive than that of the Li reference electrode, even immediately after the charge at a rate of $20 \mu\text{A cm}^{-2}$. This indicated that Li intercalation took place without deposition of Li metal on the Li_xC_6 electrode. The most serious problem with the Li-ion cell is that upon continuous charging beyond 20% of the capacity, the cell voltage and the potential of the Li_3TiS_2 electrode began to rise simultaneously, leading to the deterioration of the cycle characteristics. The polarization is probably associated not with the irreversible decomposition of electrolyte but with slow diffusion of Li in the Li_3TiS_2 electrolyte-electrode mixture, because no permanent increase in cell resistance was observed in the subsequent discharge. Further optimization studies on the cell design and the electrode mixtures have to be made to improve utilization and cycleability. To our knowledge, the cell presented here is the first solid-state Li-

ion cell working at ambient temperature, based on polycrystalline materials including carbon materials, and that is fabricated simply by pressing powdered electrolyte and electrode materials.

4. Conclusions

New intermediate compounds $3\text{Li}_3\text{N-MI}$ ($\text{M} = \text{Li}, \text{Na}, \text{K}, \text{Rb}$) were found in the quasi-binary systems $\text{Li}_3\text{N-MI}$. They were isomorphous and had a tetragonal unit cell. Their sintered bodies exhibited high Li-ion conductivity of 1.1×10^{-4} – $7.0 \times 10^{-5} \text{ S cm}^{-1}$ at room temperature. The grain boundary resistances were negligibly small because of their good sinterability. The decomposition voltages were approximately 2.5–2.8 V, much higher than that of Li_3N . Even the compacts of the powdered compounds showed total conductivities more than $10^{-5} \text{ S cm}^{-1}$. This allowed the cell construction of the solid-state Li-ion cell, $\text{C}/3\text{Li}_3\text{N-KI}/\text{LiTiS}_2$, simply by pressing the powdered electrolyte and electrode materials. The cell was able to charge and discharge at a constant current of $15 \mu\text{A cm}^{-2}$ at room temperature; however, severe polarization in the positive electrode limited the charge/discharge performance.

Acknowledgements

J.K. thanks the late Professor Y. Takaki for offering the Cell-series programs of XRD analysis, and O. Onishi and I. Baba for building the software for a.c. impedance measurement. Thanks also due to Y. Suzuki and Y. Kagawa for their experimental assistance.

References

- [1] J.M. Tarascon, Special Issue, Recent Advances in Rechargeable Li Batteries *Solid State Ionics*, 69 (1994) 295–305.
- [2] G. Pistoia (ed.), *Lithium Batteries*, Elsevier, Amsterdam, 1994.
- [3] T. Mohri, N. Yanagisawa, Y. Tajima, H. Tanaka, T. Mitate, S. Nakajima, M. Yodhida, Y. Yoshimoto, T. Suzuki and H. Wada, *J. Power Sources*, 26 (1989) 545–551.
- [4] R. Kanno, Y. Takeda, T. Ichikawa, K. Nakanishi and O. Yamamoto, *J. Power Sources*, 26 (1989) 535–543.
- [5] T. Nagaura and K. Tozawa, *Prog. Batteries Solar Cells*, 9 (1990) 209–217.
- [6] D. Guyomard and J.M. Tarascon, *J. Electrochem. Soc.*, 139 (1992) 937–948.
- [7] J. Kuwano and A.R. West, *Mater. Res. Bull.*, 15 (1980) 1661–1667.
- [8] A.R. Rodger, J. Kuwano and A.R. West, *Solid State Ionics*, 15 (1985) 185–198.
- [9] H. Aono, E. Sugimoto, Y. Sadaoka, N. Imanaka and G. Adachi, *J. Electrochem. Soc.*, 137 (1990) 1023–1027.
- [10] J. Kuwano, N. Sato, M. Kato and K. Takano, *Solid State Ionics*, 70/71 (1994) 332–336.
- [11] Y. Inaguma, C. Liqun, M. Itoh, T. Nakamura, T. Uchida, H. Ikuta and M. Wakihara, *Solid State Commun.*, 86 (1993) 689–693.
- [12] H. Kawai and J. Kuwano, *J. Electrochem. Soc.*, 141 (1994) L78–L79.

- [13] B.A. Boukamp and R.A. Huggins, *Mater. Res. Bull.*, *13* (1978) 23–32.
- [14] U.V. Alpen, M.F. Bell and T. Gladden, *Electrochim. Acta*, *24* (1979) 741–744.
- [15] J.R. Rea and D.L. Foster, *Mater. Res. Bull.*, *14* (1979) 841–846
- [16] P. Hartwig, W. Wepner and W. Wichelhaus, in P. Vashishta, J.N. Mundy and G. Shenoy (eds.), *Fast Ion Transport in Solids*, North-Holland, Amsterdam, 1979, pp. 487–490.
- [17] H. Obayashi, R. Nagai, A. Gotoh, S. Mochizuki and T. Kudo, *Mater. Res. Bull.*, *16* (1981) 587–590.
- [18] M.Z.A. Munshi and B.B. Owens, in A.L. Laskar and S. Chandra (eds.), *Superionic Solids and Solid Electrolytes*, Academic Press, San Diego, CA, 1989, pp. 641–652
- [19] I.M. Hodge, M.D. Ingram and A.R. West, *J. Electroanal. Chem.*, *74* (1976) 125–143.
- [20] Y. Takaki, T. Tamiguchi and H. Hori, *J. Ceram. Soc. Jpn.*, *101* (1993) 373–376.
- [21] F.K. McTaggart and A.D. Wadsley, *Aust. J. Chem.*, *11* (1958) 445–456.
- [22] M.B. Dienes, *Mater. Res. Bull.*, *10* (1975) 287–292